

Controllable binding of polar molecules and meta-stability of 1-D gases with attractive dipole forces

Jason N. Byrd,* John A. Montgomery, Jr., and Robin Côté
Department of Physics, University of Connecticut, Storrs, CT 06269

We explore one-dimensional (1-D) samples of ultracold polar molecules with attractive dipole-dipole interactions and show the existence of a repulsive barrier due to a strong quadrupole interaction between molecules. This barrier can stabilize a gas of ultracold KRb molecules and even lead to long-range wells supporting bound states between molecules. The properties of these wells can be controlled by external electric fields, allowing the formation of long polymer-like chains of KRb, and studies of quantum phase transitions by varying the effective interaction between molecules. We discuss the generalization of those results to other systems.

PACS numbers:

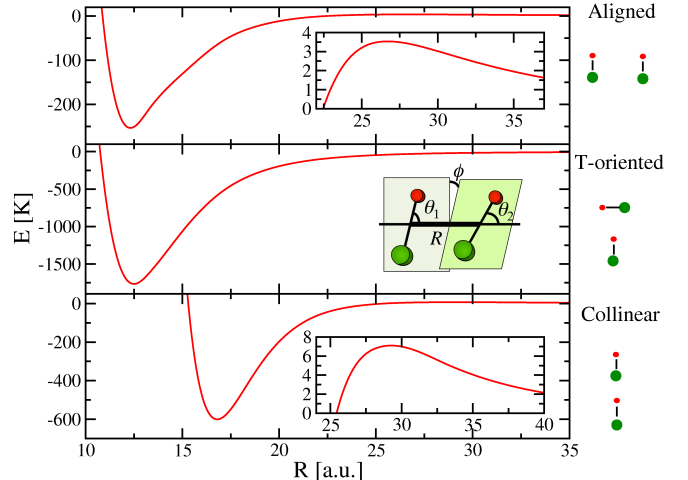
The recent achievements in the formation and manipulation of ultracold polar molecules [1, 2] have opened the gate to exciting new studies in several fields of physical sciences. Polar molecules could find uses in quantum information [3] and precision measurements [4], while their long-range and anisotropic interactions in dense samples could provide a fertile ground for novel quantum gases [5]. In addition, advances in controlling the alignment and orientation of polar molecules [6, 7] enable the manipulation of these inter-molecular interactions, building a bridge between atomic, molecular, and optical (AMO) physics, physical chemistry, and condensed matter physics. Until now, stable dipolar gases were thought to require a repulsive dipole-dipole interaction, such as provided by parallel dipoles perpendicular to a 2-D plane. However, to observe interesting new correlations and phases, such as the Luttinger liquid transition [8] attractive interactions are needed. In this work, a system with such features is proposed and investigated, combining available techniques to produce ultracold polar molecules with the ability to precisely control their spatial orientation.

In this work, we focus our attention on KRb, which has been trapped in relatively large amounts [1]. We first calculate the potential energy surface (PES) $V(R, \theta_1, \theta_2, \phi)$ of two KRb molecules approaching each other for a wide range of geometries. We assume that both molecules are in the ro-vibrational ground state of their electronic $X^1\Sigma^+$ ground state, and rigid rotors, an approximation that is valid for $R \sim 20$ a.u. (with the bond stretching by less than 0.15%) or larger. Fig. 1 shows the PES for three particular geometries when both molecular axes are in the same plane ($\phi = 0$): the top panel depicts V when the molecules are aligned ($\theta_1 = \theta_2 = 90^\circ$), the middle panel for the T -orientation ($\theta_1 = 0, \theta_2 = 90^\circ$), and the bottom panel for collinear molecules ($\theta_1 = \theta_2 = 0$). Those curves illustrate the difference between the stronger short-range region where the electronic wavefunction becomes perturbed and the weaker long-range region where the bond length of each KRb is not affected. The short-range region is generally deep, with wells that depend strongly

on the particular geometry, ranging from a few 100 K in Fig. 1 for co-planar geometries, to the tetramer K_2Rb_2 bound by ~ 4300 K with respect to the $KRb+KRb$ threshold [9].

The $KRb+KRb$ PES was calculated at the CCSD(T) level of theory using MOLPRO 2009.1 [10, 11], with the K and Rb core electrons replaced by the Stuttgart relativistic ECP18SDF [12] and ECP36SDF [13] pseudopotentials, respectively. The core-core and core-valence correlation energy was modeled using a core polarization potential [12]. Supplemental basis functions were added to existing basis sets for K [14] and Rb [15]. Uncontracting the basis sets, the exponents were optimized to reproduce the experimental equilibrium bond length, R_e , and dissociation energy, D_e [16]. In the long-range region where the interaction is small and the wave function overlap between the two molecules is negligible, the interaction can be split into electrostatic and dispersion contributions.

FIG. 1. $KRb+KRb$ PES for coplanar geometries: aligned (top), T -oriented (middle), and collinear (bottom). The inset sketches the geometry: \mathbf{R} joins the geometric center two KRb, θ_1 and θ_2 are the angles between their molecular axes and \mathbf{R} , and ϕ is the angle between the molecular planes.



Our analysis is concentrated on the coplanar geometries of Fig. 1, which depict a seemingly surprising result. While the top and middle panels depict the expected behavior of a repulsive and slightly attractive dipole-dipole interaction, respectively, the collinear geometry (bottom panel) reveals a barrier. The existence of this barrier can be traced to a strong repulsive quadrupole interaction (see below). We also notice that it is higher (almost 7 K in height) than that of the aligned geometry (about 4 K). To better understand these *ab initio* results, we examine the KRb+KRb interaction at large intermolecular separation R *via* the long-range expansion

$$V(R, \theta_1, \theta_2, \phi) \stackrel{R \text{ large}}{\simeq} - \sum_n \frac{W_n(\theta_1, \theta_2, \phi)}{R^n}. \quad (1)$$

The functions W_n may contain electrostatic (*e.g.* dipole \mathcal{D} , quadrupole \mathcal{Q} , octupole \mathcal{O} , or higher-order moments) and/or dispersion and induction contributions $C_{n,i}$ [17]. The first few terms (up to $n = 6$) are

$$\begin{aligned} W_3 &= \mathcal{D}^2 (2c_1c_2 - s_1s_2c_\phi), \\ W_4 &= \frac{3\mathcal{D}\mathcal{Q}}{2} (1 + 3c_1c_2 - 2s_1s_2c_\phi) (c_1 - c_2), \\ W_5 &= \mathcal{D}\mathcal{O} \left\{ \frac{3}{2}s_1s_2c_\phi(2 - 5c_1^2 - 5c_2^2) - c_1c_2(6 - 5c_1^2 - 5c_2^2) \right\} \\ &\quad - \mathcal{Q}^2 \left\{ \frac{3}{2}(1 - 3c_1^2)(1 - 3c_2^2) - 12c_1c_2s_1s_2c_\phi + \frac{3}{4}s_1^2s_2^2c_{2\phi} \right\}, \\ W_6 &= C_{6,0} + C_{6,1}(3c_1^2 + 3c_2^2 - 2) + C_{6,2}(3c_1^2 - 1)(3c_2^2 - 1) \\ &\quad + C_{6,3}c_1c_2s_1s_2c_\phi + C_{6,4}s_1^2s_2^2c_{2\phi} \end{aligned}$$

where $c_i \equiv \cos \theta_i$, $s_i \equiv \sin \theta_i$, $c_{k\phi} \equiv \cos k\phi$. In Table I, we list the corresponding parameters obtained by least squares fit of the PES up to $n = 8$. The fitted \mathcal{D} , \mathcal{Q} , and \mathcal{O} are also compared to *ab initio* values calculated at the all electron CCSD level of theory with the Roos ANO basis set [18]. \mathcal{D} and \mathcal{Q} agree to better than 1%, attesting to the accuracy of the PES, while \mathcal{O} is off by one order of magnitude, reflecting the difficulty of fitting the small contribution of $\mathcal{D}\mathcal{O}$ compared to that of \mathcal{Q}^2 in W_5 ($\mathcal{D} \ll \mathcal{Q}$); \mathcal{O} does not play a significant role for KRb. Using Eq.(1), one can easily understand the physical origin of the barriers. For parallel molecules, *i.e.* $\theta_1 = \theta_2 \equiv \theta$ and $\phi = 0$, the two leading terms in V are

$$V(R, \theta) \simeq -\frac{W_3}{R^3} - \frac{W_5}{R^5}. \quad (2)$$

For collinear KRb, $\theta = 0$, with $W_3 = 2\mathcal{D}^2$ and $W_5 = -6\mathcal{Q}^2 + 4\mathcal{D}\mathcal{O} \simeq -6\mathcal{Q}^2$, and because of the relatively weak \mathcal{D} when compared to \mathcal{Q} , the long-range attractive R^{-3} dipole interaction is overcome by a shorter-range repulsive R^{-5} quadrupole interaction (the attractive contribution of $\mathcal{D}\mathcal{O}$ is much weaker than that of the repulsive \mathcal{Q}^2); at shorter range still, the attractive R^{-6} and higher contributions dominate (mostly due to the

KRb fit	AB	R_e	\mathcal{D}	\mathcal{Q}	\mathcal{O}	W_6	R_{sr}	R_Q
\mathcal{D} 0.234	KRb	7.69	0.234	16.99	-3.16	18,528	10.7	126
\mathcal{Q} 17.06	LiNa	5.45	0.246	10.56	-1.80	4,265	6.34	74.4
\mathcal{O} -23.71								
$C_{6,0}$ 11679	RbCs	8.37	0.554	14.19	-5.39	26,599	21.6	44.6
$C_{6,1}$ 3182								
$C_{6,2}$ 10441	LiRb	6.50	1.715	11.80	-1.61	8,528	9.95	12.0
$C_{6,3}$ -2893	LiCs	6.93	2.335	11.00	-7.26	10,951	12.7	8.5
$C_{6,4}$ 158	NaK	6.61	1.199	12.91	3.83	9166	9.52	18.5

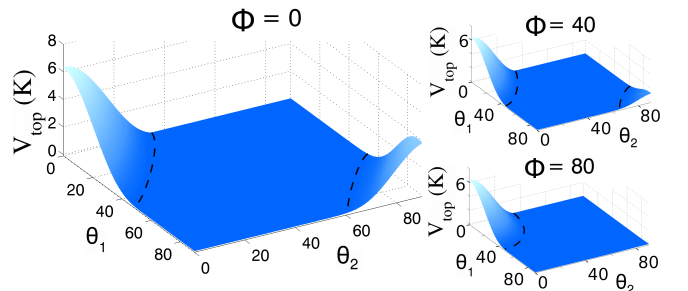
TABLE I. Left: fit parameters (up to R^{-6}). Right, *ab initio* values of the equilibrium separation R_e , moments \mathcal{D} , \mathcal{Q} , and \mathcal{O} (from the geometric center), W_6 for the collinear orientation, and the turning points R_{sr} and R_Q for various molecules AB in $v = 0$ of $X^1\Sigma^+$. All values are in atomic units.

isotropic $C_{6,0}$ term) and bring V down, hence the barrier. For aligned KRb, $\theta = 90^\circ$, with $W_3 = -\mathcal{D}^2$ and $W_5 = -(9/4)\mathcal{Q}^2 + 3\mathcal{D}\mathcal{O} \simeq -(9/4)\mathcal{Q}^2$, and although both leading contributions are repulsive, the leading repulsive W_5 is about 3 times smaller than for the collinear case, hence the smaller barrier shown in Fig. 1 (the leading attractive $C_{6,0}$ term is the same in both cases).

Using Eq. (1), we study the geometries leading to a long-range barrier; Fig. 2 depicts its height V_{top} as a function of θ_1 and θ_2 for a few twist angles ϕ . For $\phi = 0$, a substantial barrier exists along the diagonal $\theta \equiv \theta_1 = \theta_2$, for small angles ($\theta \sim 20^\circ$ or less), and for large angles ($\theta \sim 70^\circ$ or more). While the barrier remains present for the small angle cone ($\sim 20^\circ$) as ϕ increases, it quickly disappears for large θ . Roughly speaking, there is a barrier for a cone of $\theta \sim 20^\circ$ for any ϕ , and for larger molecular misalignment, the barrier vanishes. A significant barrier can thus be maintained by aligning the molecules within a small angular cone, allowing ultracold KRb samples to remain stable and even be evaporatively cooled in various trap geometries (1-D when nearly collinear, and 1-D or 2-D when nearly aligned).

Polar molecules can be oriented by coupling rotational states along a polarizing external electric field \mathbf{F} . This can be achieved by using a DC electric field; however the small dipole moment of KRb requires field strengths that

FIG. 2. V_{top} vs. θ_1 and θ_2 . The main plot corresponds to a twist angle $\phi = 0$, while the two smaller plots to $\phi = 40^\circ$ (top) and 80° (bottom). V_{top} is set to zero if there is no barrier.



are difficult to achieve in the laboratory. An alternative is to add a separate polarizing laser field [19] that directly couples the rotational states of the molecule. Although this requires a much smaller DC field, non-adiabatic effects are prominent [6], and for the sake of simplicity we calculate the rotational state coupling through directly scaling the external field. In the rigid-rotor approximation, we get a superposition of field-free symmetric top states

$$|\tilde{J}\tilde{M}\tilde{\Omega}\rangle = \sum_{J,M} a_{M,\tilde{M}}^{J,\tilde{J}} |JM\Omega\rangle \quad (3)$$

labeled by their total angular momentum J with projection M along \mathbf{F} . After transforming the molecule-fixed frame potential $V(R, \theta_1, \theta_2, \phi)$ to the laboratory-fixed frame $V_{\text{Lab}}(\mathbf{R}, \hat{r}_1, \hat{r}_2)$ [20], the field averaged potential is found by evaluating

$$V(\mathbf{R}) = \langle \tilde{J}'\tilde{M}'\tilde{\Omega}' | V_{\text{Lab}}(\mathbf{R}, \hat{r}_1, \hat{r}_2) | \tilde{J}\tilde{M}\tilde{\Omega} \rangle. \quad (4)$$

In Fig. 3, we illustrate the effect of \mathbf{F} on a pair of KRb molecules in 1-D, with θ_F defined as the angle between \mathbf{F} and \mathbf{R} . For weak fields ($F \lesssim 10$ kV/cm), the molecules remain largely in their $J = 0$ rotational state, the field mixes only small amounts of higher J states. Classically, they precess “wildly” on a wide cone about \mathbf{F} , and thus the KRb+KRb interaction samples a large range of relative angles, averaging its attractive and repulsive components, with the main contribution arising mainly from the isotropic attractive van der Waals $C_{6,0}$ term. This is depicted by the dashed lines in Fig. 3(a) with a field of 5 kV/cm for the aligned (left) and collinear (right) orientations. In both cases, the interaction becomes strongly attractive at short distance, with the aligned geometry having a weak barrier (~ 1 mK) and the collinear case showing no sign of a barrier. The solid lines show the effect of a larger electric field of 200 kV/cm; \mathbf{F} strongly mixes many (~ 7) more J 's and classically the molecules precess on a tighter cone, sampling a more restrictive range of angles. The anisotropic interactions do not average to zero, and strong barriers are present for both aligned and collinear cases. Fig. 3(b) shows the interaction for a range of θ_F near the aligned and collinear orientations for $F = 200$ kV/cm. Since the molecules then behave almost like rigid rods, we recover results similar to those in the molecular-frame. The barrier survives for a cone of angle θ_F of about 20° for both orientations, and the same conclusions about stability of 1-D and 2-D samples apply. For the aligned orientation, the barrier appears rapidly even for low fields, while larger fields ($F \gtrsim 70$ kV/cm) are necessary for the collinear case (see Fig 3(c)). In both cases, the barrier grows rapidly to hundreds of mK, a value much higher than the typical kinetic energy of the trapped ultracold molecules (< 100 μ K).

Fig. 3(b) hints at the existence of a long-range well for the collinear geometry. We analyze this well in the

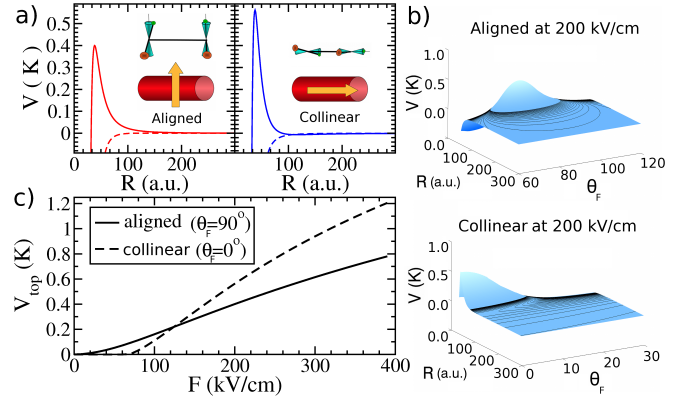


FIG. 3. (a) KRb+KRb interaction (1-D) for weak (5 kV/cm: dashed lines) and strong electric fields (200 kV/cm: solid lines), oriented perpendicular (left) and parallel (right) to the intermolecular axis. The red cylinder represents the 1-D trap, the arrow the orientation of the field, and the sketch above the precessing molecules. (b) Intermolecular interaction with $F = 200$ kV/cm for the aligned (top) and collinear (bottom) geometries as a function of θ_F (angle between \mathbf{F} and \mathbf{R}). (c) Height of the barrier for the aligned and collinear orientations as a function of F .

limit of infinite electric field, when the molecules are fully parallel ($\theta \equiv \theta_1 = \theta_2$ and $\phi = 0$) and both molecular-frame and laboratory-frame (for 1-D trapped molecules) potentials coincide ($\theta = \theta_F$). We find a long-range well that can sustain several bound levels due to its large extension and the large mass of the KRb molecules. For $\theta = 0$, there are 7 levels, the deepest bound by nearly 2.7 mK with inner and outer classical turning points at 110 a.u. and 205 a.u., respectively. As θ increases, the barrier due to the R^{-5} repulsion gets smaller and the well deepens, and the binding energies increase accordingly until θ reaches $\theta_c \simeq 22^\circ$, at which point the barrier disappears and no more long-range bound levels exist (see Fig. 4(a)). We note that for a small deviation from $\theta = 0$, the binding energies are not significantly affected, and an additional level $v = 7$ appears for $18^\circ < \theta < \theta_c$ (inset in Fig. 4(a)).

The variation of bound levels with θ affects the scattering between molecules and their effective interaction. Assuming θ (or θ_F) as a fixed external parameter, we estimate the s -wave scattering phase shift δ between two KRb, which depends on the interaction V and the wave number k ; $\delta < 0$ (> 0) corresponds to an effective repulsive (attractive) interaction. Here, we choose k assuming $\hbar^2 k^2 \sim m k_B T$ (m : mass of KRb; k_B : Boltzmann constant) for $T \simeq 700$ nK [1] and illustrate the effect in Fig. 4(b) for the infinite field case (*i.e.* $\theta_F = \theta$). For angles smaller than $\sim 14.7^\circ$, the interaction is attractive (with $\delta > 0$), while it becomes repulsive ($\delta < 0$) for larger angles. In an ideal 1-D trap, the repulsive barrier at $R \sim 100$ a.u. would stabilize the sample for an attractive effective interaction by preventing the molecules

from reaching short distances where inelastic processes (*e.g.*, chemical reactions) could take place. Larger angles, but still within the stability cone, would also give stable samples since the effective interaction is repulsive. By varying the orientation of the electric field with respect to the trap axis, the behavior of the sample could be controlled; an effective attractive interaction would lead to a dense self-trapped system, *i.e.* a liquid-like sample, while an effective repulsive interaction would give a dilute sample behaving like a gas. Such control could probe a quantum phase transition between a Luttinger liquid and an ultracold gas [8]. One could also create a chain of KRb molecules weakly bound together (*e.g.* by using photoassociation); these would be akin to ultracold polymer-like chains stabilized by an external electric field and a 1-D trap. We note that the effective interaction can also be controlled by varying the magnitude of \mathbf{F} . In Fig. 4(c), we show δ for $\theta_F = 0$ as a function of F for two collision energies corresponding to 700 nK and 900 nK, and find that its sign can be changed by varying F .

Obtaining 1-D traps is challenging; assuming a harmonic trap in the perpendicular direction characterized by the frequency ω , the size of the ground state $a \sim \sqrt{\hbar/m\omega}$ is of the order of a few 1000 a.u. for optical traps. Molecules at densities of 10^{12} cm^{-3} loaded in such traps would be separated by roughly $d \sim 1 \mu\text{m}$, and for repulsive effective interaction, the angle $\tan^{-1} a/d \lesssim 10^\circ$ between their axes would remain within the cone of stability. For an attractive effective interaction, the relevant angle is $\tan^{-1} a/R_Q$, where R_Q is the point where the barrier begins for two approaching molecules (see below), which requires $a \sim 0.4R_Q = 50 \text{ a.u.}$ for KRb. Here, the sample would not be 1-D, with inelastic processes possibly taking place. Non-reactive species, such as RbCs (see below), could be considered to prevent inelastic processes, or much tighter magnetic traps could be employed; in which case molecules in a triplet electronic state with a magnetic moment μ would be required. For KRb in its $a^3\Sigma^+(v=0)$ state, $a \sim 60 \text{ a.u.}$ can be achieved [21], and with $R_Q \sim 150 \text{ a.u.}$ [22], $\tan^{-1} a/R_Q$ would remain within the stability cone.

The features discussed here for KRb can be generalized to other polar molecules. The PES at long-range is well described by (1), and the existence of a barrier for perfectly collinear molecules depends mostly on the first two terms (see Eq.(2)). By setting $V = 0$ and neglecting \mathcal{DQ} , we find $R_Q \simeq \sqrt{3Q^2/\mathcal{D}^2}$, the point where the R^{-5} repulsion takes over the R^{-3} attraction. We can also define a point R_{sr} where the shorter range R^{-6} attraction takes over the R^{-5} repulsion, by neglecting the other contributions and setting $V \sim -W_5/R^5 - W_6/R^6 = 0$, which gives $R_{\text{sr}} = -W_6/W_5$. If R_Q is outside the region where bonds are strongly perturbed ($\sim 20 \text{ a.u.}$) or higher W_n terms contribute significantly (roughly R_{sr}), then the barrier can exist. Table I gives R_Q and R_{sr} for various polar molecules. Because Q has roughly the same am-

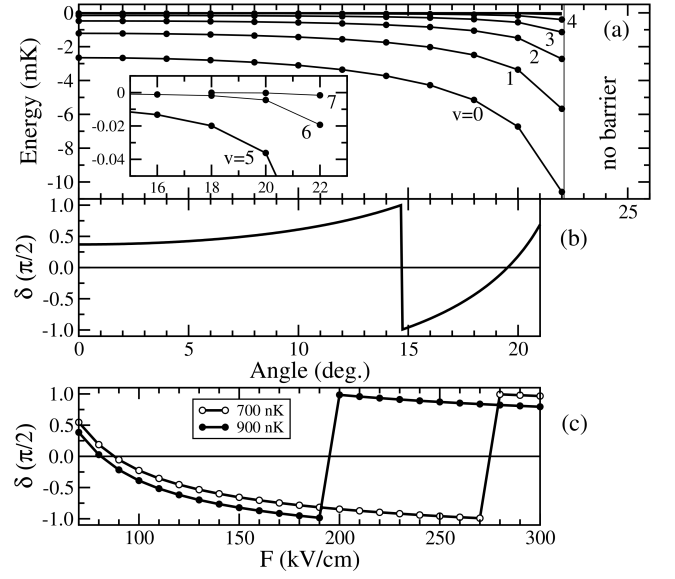


FIG. 4. (a) Long-range well energy levels vs. θ ; an additional level $v = 7$ appears at 18° (inset). (b) scattering phase shift δ vs. θ for k corresponding to 900 nK for infinite F . (c) δ for $\theta_F = 0$ as a function of the field strength F for collision energies corresponding to 700 nK and 900 nK.

plitude for most of them, \mathcal{D} dictates the behavior of the systems. Molecules with small \mathcal{D} (*e.g.*, LiNa and KRb) have a sizable R_Q , and thus the existence of a barrier is very likely, unlike those with a large \mathcal{D} (*e.g.*, LiRb, LiCs and NaK). We also include RbCs, for which the existence of a barrier is uncertain. This is interesting since RbCs is known to not be reactive. However, a full investigation is required to know if a barrier exists.

In conclusion, we found that the interaction between polar molecules exhibits a strong barrier when they are oriented about two specific geometries: aligned and collinear. We also showed that the collinear setting gives meta-stable samples of ultracold molecules in a tight 1-D trap. The long-range R^{-3} dipolar attractive and R^{-5} quadrupolar repulsive contributions in the collinear geometry lead to long-range wells between polar molecules sustaining several bound levels. Varying the orientation of the molecules using an external electric field allows for non-trivial effects, such as changing the effective interaction from repulsive to attractive, and possibly the phase of the sample from gas to liquid. Finally, we also predict the existence of the collinear barrier for various bi-alkali polar molecules based on the relative strength of the dipole and quadrupole moments. The combination of available techniques to produce ultracold molecules [1, 2] and the ability to precisely control their spatial orientation [6, 7] provide the tools to investigate such systems.

The authors wish to thank H. Harvey Michels and Jörg Schmiedmayer for useful discussions. This work was supported in part by the Department of Energy, Office of Basic Energy Sciences and the AFOSR MURI grant on

ultracold polar molecules.

* byrd@phys.uconn.edu

- [1] M. de Miranda, A. Chotia, B. Neyenhuis, D. Wang, G. Quémener, S. Ospelkaus, J. Bohn, J. Ye, and D. Jin, *Nature Physics* **7**, 502 (2011)
- [2] J. Deiglmayr, M. Repp, R. Wester, O. Dulieu, and M. Weidemüller, *Phys. Chem. Chem. Phys.* **13**, 19101 (2011)
- [3] S. F. Yelin, K. Kirby, and R. Côté, *Phys. Rev. A* **74**, 050301(R) (2006)
- [4] D. DeMille, F. Bay, S. Bickman, D. Kowall, D. Krause, S. Maxwell, and L. Hunter, *Phys. Rev. A* **61**, 052507 (2000)
- [5] L. Santos, G. Shlyapnikov, P. Zoller, and M. Lewenstein, *Phys. Rev. Lett.* **85**, 1791 (2000)
- [6] J. Nielsen, H. Stapelfeldt, J. Küpper, B. Friedrich, J. Omiste, and R. González-Férez, *Phys. Rev. Lett.* **108**, 193001 (2012)
- [7] L. Holmegaard, J. Nielsen, I. Nevo, H. Stapelfeldt, F. Filsinger, J. Kupper, and G. Meijer, *Phys. Rev. Lett.* **102**, 023001 (2009)
- [8] A. Recati, P. Fedichev, W. Zwerger, and P. Zoller, *Phys. Rev. Lett.* **90**, 020401 (2003)
- [9] J. N. Byrd, J. A. Montgomery, Jr., and R. Côté, *Phys. Rev. A* **82**, 010502(R) (2010)
- [10] H. J. Werner, P. J. Knowles, R. Lindh, F. R. Manby, M. Schütz, *et al.*, “Molpro, version 2009.1, a package of ab initio programs,” (2009)
- [11] P. J. Knowles, C. Hampel, and H. J. Werner, *J. Chem. Phys.* **99**, 5219 (1993)
- [12] P. Fuentealba, H. Preuss, H. Stoll, and L. V. Szentpály, *Chem Phys Lett* **89**, 418 (1982)
- [13] P. Fuentealba, H. Stoll, L. v. Szentpaly, P. Schwerdtfeger, and H. Preuss, *J. Phys. B* **16**, L323 (1983)
- [14] S. Magnier and P. Millie, *Phys. Rev. A* **54**, 204 (1996)
- [15] M. Aymar and O. Dulieu, *J. Chem. Phys.* **122**, 204302 (2005)
- [16] A. Pashov, O. Docenko, M. Tamanis, R. Ferber, H. Knöckel, and E. Tiemann, *Phys. Rev. A* **76**, 022511 (2007)
- [17] F. Mulder, A. van der Avoird, and P. E. S. Wormer, *Mol. Phys.* **37**, 159 (1979)
- [18] B. Roos, V. Veryazov, and P.-O. Widmark, *Theor. Chem. Acc.* **111**, 345
- [19] M. Härtelt and B. Friedrich, *J. Chem. Phys.* **128**, 224313 (2008)
- [20] T. V. Tscherbul, Y. V. Suleimanov, V. Aquilanti, and R. V. Krems, *New J. Phys.* **11**, 055021 (2009)
- [21] R. Folman, P. Krüger, J. Schmiedmayer, J. Denschlag, and C. Henkel, *Adv. At. Mol. Opt. Phys.* **48**, 263 (2002)
- [22] $\mathcal{D} = 0.017$ a.u. and $\mathcal{Q} = 1.47$ a.u. were computed at the same level of theory mentioned in the text, leading to $R_Q \sim 150$ a.u. for KRb.